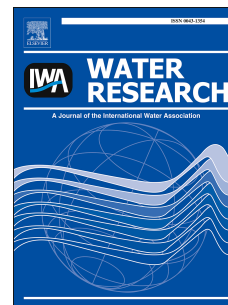


# Journal Pre-proof

Effect of cathode material and charge loading on the nitrification performance and bacterial community in leachate treating Electro-MBRs

Dany Roy, Patrick Drogui, Mohamed Rahni, Jean-François Lemay, Dany Landry, Rajeshwar D. Tyagi



PII: S0043-1354(20)30527-3

DOI: <https://doi.org/10.1016/j.watres.2020.115990>

Reference: WR 115990

To appear in: *Water Research*

Received Date: 20 February 2020

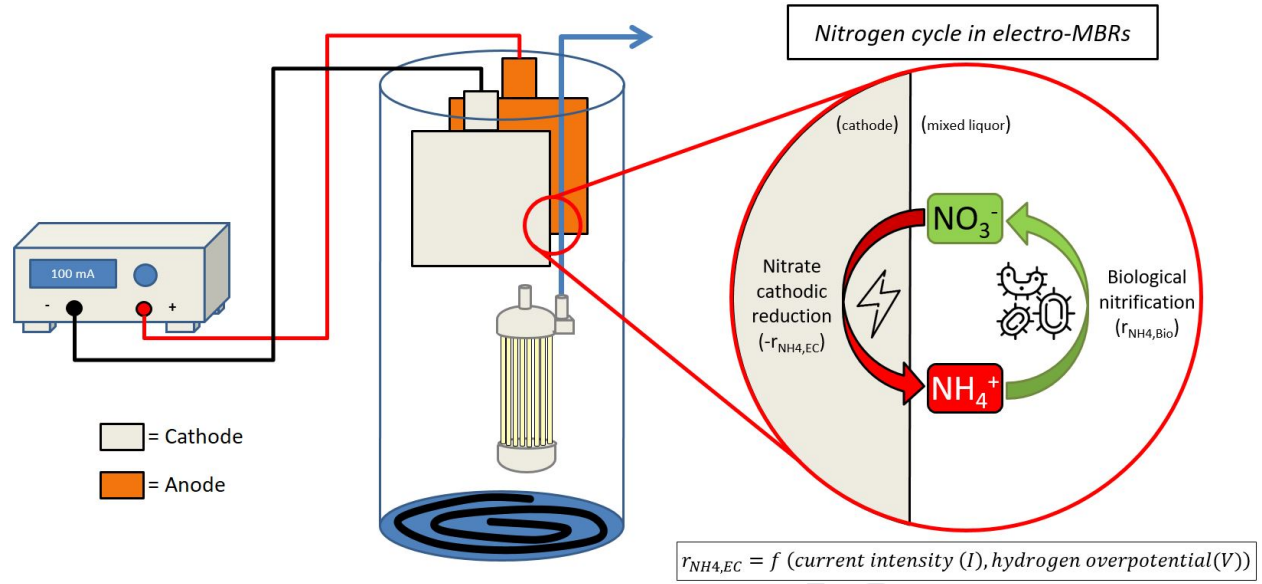
Revised Date: 3 May 2020

Accepted Date: 27 May 2020

Please cite this article as: Roy, D., Drogui, P., Rahni, M., Lemay, Jean.-Franç., Landry, D., Tyagi, R.D., Effect of cathode material and charge loading on the nitrification performance and bacterial community in leachate treating Electro-MBRs, *Water Research* (2020), doi: <https://doi.org/10.1016/j.watres.2020.115990>.

This is a PDF file of an article that has undergone enhancements after acceptance, such as the addition of a cover page and metadata, and formatting for readability, but it is not yet the definitive version of record. This version will undergo additional copyediting, typesetting and review before it is published in its final form, but we are providing this version to give early visibility of the article. Please note that, during the production process, errors may be discovered which could affect the content, and all legal disclaimers that apply to the journal pertain.

© 2020 Published by Elsevier Ltd.



1 Effect of cathode material and charge loading on the  
2 nitrification performance and bacterial community in  
3 leachate treating Electro-MBRs

4  
5 **Authors:**

6 *Dany Roy<sup>a,\*</sup>, Patrick Drogui<sup>a,\*</sup>, Mohamed Rahni<sup>c</sup>, Jean-François Lemay<sup>c</sup>, Dany Landry<sup>b</sup>, Rajeshwar D.*  
7 *Tyagi<sup>a</sup>*

8 <sup>a</sup> INRS, 490, rue de la Couronne, Québec, Qc., Canada, G1K 9A9

9 <sup>b</sup> Englobe Corp., 505 Boul. de Parc Technologique, Québec, Qc., Canada, G1P 4S7

10 <sup>c</sup> CNETE, 2263, Avenue du Collège, Qc, Canada, G9N 6V8

11 \* [Patrick.drogui@ete.inrs.ca](mailto:Patrick.drogui@ete.inrs.ca); [dany.roy@ete.inrs.ca](mailto:dany.roy@ete.inrs.ca)

12  
13 **Abstract:**

14 Electro-MBR technology, which combines an electrocoagulation process inside the mixed liquor of a  
15 membrane bioreactor, was studied for the treatment of a high-strength ammonia leachate ( $124 \pm 4$  mg  
16  $\text{NH}_4\text{-N L}^{-1}$ ). A lab-scale aerobic Electro-MBR was operated with a solid retention time of 45 days,  
17 hydraulic retention times of 24h and 12h, and charge loading ranging from 100 to 400  $\text{mAh L}^{-1}$ . At 400  
18  $\text{mAh L}^{-1}$ , with a combination of a Ti/Pt cathode and a sacrificial iron anode, removal percentages for  
19 ammonia nitrogen, total organic carbon, and total phosphorus were 99.8%, 38%, and 99.0%,  
20 respectively. At 400  $\text{mAh L}^{-1}$ , the estimated ferric ion dosage was 325  $\text{mg Fe}^{3+} \text{L}^{-1}$ . Experiments  
21 conducted with different cathode materials showed that previously reported inhibition phenomena may

22 result from a cathodic nitrate reduction into ammonia nitrogen. Conventional cathode materials, such as  
23 graphite, have electrochemical nitrate reduction rates of  $-0.03 \text{ mg NO}_3\text{-N mA}^{-1}$ . By comparison, when  
24 using Ti/Pt, the rate was  $-0.0045 \text{ mg NO}_3\text{-N mA}^{-1}$  (85% lower than graphite due to its low hydrogen  
25 overpotential). Charge loading tested in this study had no significant impact on both nitrification  
26 performance and microbial population diversity. However, the relative abundance of the mixed liquor's  
27 *Nitrosomonas* increased from 4.8% to 8.2% when the charge loading increased from 0 to  $400 \text{ mA}^{-1}$ .  
28 Results from this study are promising for future applications of the Ti/Pt - Iron Electro-MBR in various  
29 high-strength ammonia wastewater treatment applications.

30

31 **Keywords:** electro membrane bioreactor, electro-coagulation, nitrification, ammonia nitrogen, leachate,  
32 microbial community

33

34 *List of abbreviation*

35	AOB	Ammonia oxidizing bacteria
36	BOD <sub>5</sub>	Biological oxygen demand over a period of 5 days
37	COD	Chemical oxygen demand
38	DC	Direct current
39	DO	Dissolved oxygen
40	EC	Electro-coagulation
41	HRT	Hydraulic retention time
42	HOP	Hydrogen overpotential
43	MBR	Membrane bioreactor
44	MLVSS	Mixed liquor volatile suspended solids
45	NLR	Nitrogen loading rate
46	OLR	Organic loading rate
47	OTU	Operating taxonomic units
48	PCoA	Principal component analysis
49	PLR	Phosphorus loading rate
50	SRT	Solid retention time
51	SS	Stainless steel
52	TSS	Total suspended solids

53

## 54 *1. Introduction*

55 Waste originating leachates are known for their composition complexity and for the threat they pose to  
56 the preservation of water resources adjacent to waste management facilities. Amongst the  
57 contaminants found in these leachates, ammonia nitrogen is of primary concern due to its numerous  
58 adverse effects, such as its promotion of eutrophication, its toxicity to aquatic organisms, and the  
59 depletion of dissolved oxygen caused by the oxidation of ammonia nitrogen to nitrate (He, Xue et al.  
60 2009). Previous studies reported ammonia nitrogen concentrations in composting and landfill leachates  
61 ranging from 5 to more than 21 000 mg NH<sub>4</sub>-N L<sup>-1</sup> (Roy, Azaïs et al. 2018).

62 The treatment of these high-strength ammonia leachates has become a major concern in recent years  
63 due to their negative effect on conventional municipal wastewater biological treatment processes.  
64 Gagnaire et al. (2011) reported that even when co-treating leachate with municipal wastewater, the  
65 dilution factor is often insufficient to dilute the ammonia nitrogen concentration peaks that inhibit the  
66 microbial activity in the mixed liquor (Gagnaire, Wang et al. 2011). Consequently, treatment systems  
67 have been engineered specifically for waste originating leachates. Amongst these technologies, the  
68 membrane bioreactor (MBR) is one of the most efficient in terms of removing ammonia nitrogen from  
69 leachates. In a previous study conducted on co-composting leachates, MBRs were shown to reach  
70 ammonia nitrogen removal rates of >740 mg NH<sub>4</sub>-N L<sup>-1</sup> d<sup>-1</sup>, which corresponds to 99.8% removal (Roy,  
71 Drogui et al. 2020). The main advantage of MBRs is their excellent control over the SRT, due to the  
72 membranes that prevent the passage of microorganisms in the permeate. Such a control over the SRT  
73 allows for the proliferation of low growth rate ammonia-oxidizing bacteria (AOB) (Canziani, Emondi et al.  
74 2006) and their acclimation to the inhibitive compounds potentially found in leachates (Vuono, Regnery  
75 et al. 2016). However, membranes are also at the origin of the main drawback of MBRs: membrane  
76 fouling. Membrane fouling is mainly caused by the small size of microbial floc (Bani-Melhem and

77 Elektorowicz 2011), high concentrations of extracellular polymeric substances in the mixed liquor (Wei,  
78 Elektorowicz et al. 2012), and soluble organic substances (Borea, Naddeo et al. 2017). Furthermore,  
79 aerobic MBRs have low phosphorus removal efficacy, which can be prohibitive for leachate treatment  
80 applications. For example, Roy et al. (2020) obtained assimilation/precipitation rates ranging from 0.026  
81 to 0.041 g P/g total suspended solids (TSS) when treating co-composting leachates, which corresponds  
82 to 37% to 71% removal (Roy, Drogui et al. 2020).

83 Lee et al. (2001) made a first attempt at solving both of the aforementioned drawbacks by feeding an  
84 inorganic coagulant directly in the mixed liquor. Using alum at a molar ratio of 1.5Al:1 P, they found that  
85 alum can efficiently coagulate colloidal particles in the range of 0.1 to 2  $\mu\text{m}$ , as well as increase microbial  
86 particles' zeta potential from -14.6 to -6.8 mV, both of which lead to a significant improvement in  
87 membrane permeability. Adding alum also increased phosphorus removal by 90% through chemical  
88 precipitation. However, the formation of  $\text{AlOH}_2$  (precipitate) and its conjugated acid,  $\text{H}_2\text{SO}_4$ , led to a  
89 reduction in pH, which inhibited biological nitrification (Lee, Kim et al. 2001). Similarly, Wu et al. (2006)  
90 tested the addition of monomeric coagulants ( $\text{Al}_2(\text{SO}_4)_3$ ,  $\text{FeCl}_3$ ) and polymeric coagulants (polymeric  
91 aluminum chloride, and polymeric ferric sulfate) to control membrane fouling. Polymeric ferric sulfate  
92 was found to be the most effective in providing the highest removal percentage of supernatant organic  
93 matter as well as the greatest enlargement of sludge floc size. However, the required high coagulant  
94 dosage in mixed liquor ( $> 0.5 \text{ mM Al or Fe}$ ) quickly led to a pH drop below 7 and inhibited biological  
95 nitrification (Wu, Chen et al. 2006).

96 To overcome the acidification problems related to the addition of inorganic coagulants, researchers  
97 proposed the combined use of electrocoagulation (EC) and MBRs. Patented in 1976 by Ramirez (Ramirez  
98 1976), EC consists of the in-situ generation of multivalent metal ions (coagulants) from the  
99 electrochemical dissolution of immersed, sacrificial anodes (Ensano, Borea et al. 2016). The main  
100 advantages of EC when compared to inorganic coagulant is: 1) the reduction in materials and

101 transportation costs compared to chemical reagents, 2) the reduced sludge production due to a lower  
102 content in bound water, and 3) the simplified dosage automation (Wei, Oleszkiewicz et al. 2009). There  
103 are two main categories of electrocoagulation-MBRs (Electro-MBR): 1) external EC unit upstream of the  
104 MBR and 2) EC directly submerged in the mixed liquor with the membrane (Ensano, Borea et al. 2016).  
105 The first configuration was initially proposed by Kim et al. (2010) for the treatment of municipal  
106 wastewater in South Korea. With a 50 m<sup>3</sup>/h electro-MBR pilot unit using aluminum cathodes and  
107 anodes, they obtained total phosphorus removal efficiency of 79.9%, as opposed to 41% for a MBR  
108 without EC (Kim, Jang et al. 2010). In the same period of time, Wei et al. (2009) studied the second  
109 configuration using synthetic municipal wastewater. Also using aluminum electrodes, they found that  
110 the Electro-MBR can significantly reduce membrane fouling and improve phosphorus removal (Wei, Shi  
111 et al. 2009). Using the same Electro-MBR as Wei et al. (2009), Bani-Melhem et Elektorowicz (2011)  
112 tested the effect on treatment performance of an intermittent DC with an operational mode of 15 min  
113 ON – 45 min OFF using iron electrodes. They found that the addition of an EC system enhanced the  
114 removal of COD and PO<sub>4</sub>-P up to 96% and 98%, respectively, but reduced ammonia nitrogen removal  
115 from 97% to 70%. These results raised concerns about the application of this technology with high  
116 strength ammonia wastewaters such as leachates. According to Bani-Melhem et Elektorowicz (2011),  
117 lower nitrification activity may be caused by two factors: 1) the greater sensitivity to the applied DC field  
118 of the nitrifying bacteria; and/or 2) the accumulation of iron in the Electro-MBR, which has some  
119 inhibitory effects on the activity of nitrifying bacteria (Bani-Melhem and Elektorowicz 2011). Similarly, Li  
120 et al. (2001) previously shown that an electricity quantity of 50 mAh L<sup>-1</sup> in an activated sludge system  
121 with stainless steel (SS) electrodes reduced the nitrification rate by 50% (Li, Cao et al. 2001). Other  
122 studies reported similar inhibitive effects on mixed liquor microbial populations and nitrification  
123 performance. Wei et al. (2011) exposed mixed liquor samples to various electricity quantities for 4 hours  
124 in a batch system and found that the percentage of live cells dropped by 15% and 29% when exposed to

125 440 mAh L<sup>-1</sup> and 890 mAh L<sup>-1</sup>, respectively (Wei, Elektorowicz et al. 2011). Bani-Melhem et Smith (2012)  
126 reported a drop in ammonia nitrogen removal from 97.4% to 77.8% when adding an EC system operated  
127 with a charge loading of 680 mAh L<sup>-1</sup> and aluminum electrodes to their MBR (Bani-Melhem and Smith  
128 2012).

129 On the other hand, other studies reported contradictory effects of the EC on nitrification performance.  
130 Tafti et al. (2015) reported that nitrogen removal efficiency improved with an electricity quantity below  
131 144 mAh L<sup>-1</sup> in an Electro-MBR (iron electrodes) when compared to an unmodified MBR (Tafti, Mirzaii et  
132 al. 2015). Similarly, Borea et al. (2016) reported that the EC increased ammonia nitrogen removal by  
133 10.5% to 27% when charge loading of 15 and 40 mAh L<sup>-1</sup> were applied with an aluminum anode and a SS  
134 cathode (Borea, Naddeo et al. 2017). Li et al. (2018) and Battistelli, da Costa et al. (2018) each compared  
135 the microbial population of an Electro-MBR to that of a MBR treating the same wastewater. Li et al.  
136 (2018) found that the relative abundance of Nitrosomonas in the MBR's mixed liquor increased from  
137 1.45 to 3.12% when a 14 mAh L<sup>-1</sup> charge load was applied (Li, Dong et al. 2018). Similarly, Battistelli, da  
138 Costa et al. (2018) reported an increase in Nitrospira relative abundance from 10% to 38% as well as  
139 higher ammonia oxidizing bacteria activity (OUR-NH<sub>4</sub><sup>+</sup>) when an electric density of 10 A m<sup>-2</sup> was applied  
140 (Battistelli, Belli et al. 2019).

141 This inconsistency in the reported effects of EC systems on MBRs nitrification performances might find  
142 its origin in the selection of the cathode material and the charge loading. Dia et al. (2017) previously  
143 studied landfill leachate treatment using biofiltration followed by EC (Dia, Drogui et al. 2017).  
144 Interestingly, they reported that nitrates reacted at the cathode and formed ammonia nitrogen  
145 according to the electrochemical reduction reactions presented in Figure 1.

146 In addition, the nitrate electrochemical reduction rate was found to be correlated with the hydrogen  
147 overpotential (HOP). In an EC process, gaseous hydrogen generation is the main chemical reaction

148 occurring on the cathode's surface. However, when the cathode material HOP value is high, nitrate  
149 reduction can compete with hydrogen generation, leading to an increase in ammonia nitrogen  
150 concentration. In order to avoid ammonia nitrogen formation, Dia et al. (2017) suggested the use of  
151 Ti/Pt as the cathode material, which has a HOP of 0.95 V, compared to 1.3, 1.75, and 1.37 V for Fe, Al,  
152 and SS, respectively. When applying 500 mA h L<sup>-1</sup> on a leachate containing 300 mg NO<sub>3</sub>-N L<sup>-1</sup>, they found  
153 that the Ti/Pt cathode reduced ammonia nitrogen formation by more than 90% compared to Fe, Al, and  
154 SS electrodes. The application of these concepts is promising in terms of Electro-MBRs' applications in  
155 the treatment of high-strength ammonia nitrogen wastewaters.

156 Another challenge with leachate is the presence of high concentrations of recalcitrant organic carbon  
157 (Roy, Benkaraache et al. 2019). MBRs are efficient technologies for the removal of easily to moderately  
158 biodegradable organic carbon. However, they are limited in terms of removing leachates' recalcitrant  
159 organic carbon at hydraulic retention times below 48h when operated at SRTs of 30 to 45 days (Roy,  
160 Drogui et al. 2020). The addition of an EC process to the MBR process has been reported to increase the  
161 organic carbon removal rates in municipal wastewaters and synthetic wastewater. However, no studies  
162 have reported its effect on recalcitrant TOC from leachate, which is mostly comprised of fulvic- and  
163 humic-like substances (high aromaticity, and presence of polar functions such as carboxyl and hydroxyl  
164 groups) (Roy, Benkaraache et al. 2019).

165 The main objective of this study is to assess the potential application of Ti/Pt Electro-MBRs in the  
166 treatment of high-strength ammonia nitrogen leachates, as well as to define the effect of the EC process  
167 on nitrification and leachate contaminant removal performances (COT and total phosphorus). Since  
168 membrane fouling is largely covered in the scientific literature, the subject will not be discussed in this  
169 study. In order to reach these objectives, the nitrate electrochemical reduction hypothesis was validated  
170 by testing a graphite and a Ti/Pt cathode in a batch EC system. Then, high-strength ammonia co-  
171 composing leachate was treated using an Electro-MBR operated at hydraulic retention times (HRT) of

172 24h and 12h, and charge loading of 0, 100, 200, and 400 mAh L<sup>-1</sup>. During this study, the following  
173 contaminants were studied: ammonia nitrogen, total organic carbon (TOC), and total phosphorus (P<sub>tot</sub>).  
174 Finally, metagenomic analyses, with a focus on amoA gene expressing bacteria, were conducted on  
175 mixed liquor samples taken at each charge loading tested in order to assess the effect of the EC on the  
176 ammonia oxidizing bacteria population activity.

## 177 **2. Material and methods**

### 178 **2.1. Electrocoagulation batch reactor**

179 The experiments on the effect of the cathode material on the cathodic nitrate reduction rate were  
180 carried out in a 0.5 L parallelepiped batch reactor made of clear PVC, as presented in Figure 2a. A  
181 magnetic stirrer was used in order to create a homogeneous internal mixing. The rectangular electrodes  
182 (10 cm x 11 cm) were immersed in the reactor at 1 cm distance from one another (Figure 2b). The  
183 sacrificial anode was made of iron. Before each experiment, the anode was first polished using an  
184 abrasive paper, and then rinsed in a 5% (v:v) diluted HCl solution for 10 minutes. Two cathodes made of  
185 different materials were tested: 1) graphite, and 2) platinized titanium (Ti/Pt). Graphite was selected for  
186 its low cost and because it had not previously been tested by Dia et al. (2017) on leachates in EC systems  
187 (Dia, Drogui et al. 2017). Ti/Pt was selected for its low HOP. The electrodes were connected to a digital  
188 DC power supply (BK Precision 9184 DC power supply, 0-100V, 2A). Co-composting leachate containing  
189 128±1 mg NO<sub>3</sub>-N L<sup>-1</sup>, treated with the MBR before the addition of electrodes (Table 1, Condition #1), was  
190 used during this experiment.

### 191 **2.2. Lab-scale submerged electrocoagulation-MBR**

192 The submerged Electro-MBR lab-scale experimental set-up was designed according to figure 3a and  
193 Figure 3b.

194

195 The leachate was kept in a 50 L polyethylene tank placed in a refrigerator at 4°C in order to avoid any  
196 biological activity that could alter the leachate's composition. The 10 L reactor was made of a 146.33  
197 mm I.D. clear PVC tube (schedule 80). The leachate was fed into the reactor through a side port using a  
198 peristaltic pump (Masterflex, model #7528-10). An ultrafiltration hollow-fiber membrane module (Zee-  
199 Weed, ZW-1) was used. The total surface area of the module's membrane is 47 cm<sup>2</sup>, while the  
200 membrane's nominal pore diameter is 0.04 µm.

201 The permeate flow rate (filtration: 300 s, flux 7.4 L m<sup>-2</sup> h<sup>-1</sup>; backwash: 20 s, flux 46.4 L m<sup>-2</sup> h<sup>-1</sup>) was  
202 maintained constant during each experiment by controlling the vacuum applied to the membrane (5 to  
203 50 kPa) with a peristaltic pump (Masterflex, model #7528-10). To prevent the accumulation of a cake  
204 layer on the membrane's surface, filtration/backwash cycles were applied, and air was introduced  
205 between the membrane fibers (2.5 L air min<sup>-1</sup>) in order to create enough shear stress to dislodge most of  
206 the biofilm. Membrane module cleaning was conducted when the transmembrane pressure reached -50  
207 kPa.

208 The electrodes (sacrificial iron anode and Ti/Pt cathode) were immersed around the membrane module  
209 at 5 cm distance from one another, similar to previous studies (Bani-Melhem and Elektorowicz 2011,  
210 Borea, Naddeo et al. 2017). This distance, combined with the high conductivity of the leachate, reduced  
211 the power requirements needed to obtain the desired charge loading, while minimizing the potential  
212 inhibitive effect of an acidic/oxidation zone on the biological nitrification (Bani-Melhem and  
213 Elektorowicz 2010). The electrodes were connected to a digital DC power supply (BK Precision 9184 DC

214 power supply, 0-100V, 2A). When the voltage reached 3V, the iron anode was changed and the Ti/Pt  
215 cathode was cleaned in a 0.1M HCl solution for 1h.

216 The Electro-MBR was operated in oxic conditions (D.O. = 6 - 7 mg O<sub>2</sub> L<sup>-1</sup>) at room temperature (20±1°C).  
217 Compressed air was introduced through a perforated tube placed at the bottom in the reactor (2.5 L  
218 min<sup>-1</sup>) and arranged in such way as to create a homogeneous internal mixing of the reactor from the  
219 rising bubbles. SRT was controlled by purging mixed liquor from the reactor on a daily basis. HRT was  
220 controlled by adjusting the mixed liquor volume; it was calculated by measuring the collected permeate  
221 and mixed liquor volume on a daily basis.

### 222 **2.3. Experimental procedure**

223 Over the course of the experiment's 70-day duration, three different charge loading (100, 200, and 400  
224 mAh L<sup>-1</sup>) were tested at a constant SRT of 45 days. The electric current was applied with a continuous  
225 operation mode. The details of the experimental conditions are presented in Table 1.

226 The charge loading ( $\dot{q}$ ) is defined by the amount of electricity transferred through electrochemical  
227 reaction for a given amount of water treated, and it is calculated using the following equation (Eq. 1):

$$\dot{q} = \frac{I}{V} * HRT \quad \text{Eq. 1}$$

228 Where I is the applied current (mA), V is the reactor's volume (L), and the HRT is expressed in hours. The  
229 mixed liquor used in this study originated from a previous experiment in which the MBR (without  
230 electrodes) was operated at a HRT of 45 days during 60 days with composting leachate collected in the  
231 same composting facility as were collected this study's leachate (St-Henri-de-Lévis's composting facility,  
232 Canada) (Roy, Drogui et al. 2020). In order to adapt the mixed liquor's microbial population to this  
233 study's leachate contaminant concentrations, the MBR was initially operated without applied current for  
234 28 days (Condition #1). Then, the three different applied charge loading were maintained for 14 days

235 each (Conditions #2, #3 and #4) in order to reach steady-state conditions and to provide an adequate  
236 duration for sample collection. After 10 days of operation under the same operating conditions, samples  
237 were taken every day for 4 days. If the difference in TOC and  $\text{NH}_4^+$  removal rates, as well as MLVSS  
238 between two samples taken within a 4-day interval was less than 5%, then the MBR was considered to  
239 be operating at steady-state. The characterization of the co-composting leachate treated in this study is  
240 presented in Table 2.

## 241 **2.4. Analytical methods**

### 242 **2.4.1. Microbial community analysis**

#### 243 **Genomic DNA extraction**

244 Genomic DNA was extracted from 10 ml of each sample using a DNeasy Powersoil kit following the  
245 manufacturer's protocol (Quiagen). The final elution volume was 100  $\mu\text{l}$ , and the concentration was  
246 determined with the Quant-it Picogreen kit (Thermofisher) and the NanoDrop 330 Fluorospectrometer  
247 (thermofisher).

#### 248 **Illumina MiSeq**

249 The first PCR amplifications were performed with the primer Bakt\_341F (5'-CCTACGGGNGGCWGCAG-3')  
250 and the primer Bakt\_805R (5'-GACTACHVGGGTATCTAATCC-3'), designed by Herlemann et al. (2011)  
251 (Herlemann, Labrenz et al. 2011). Common sequence 1 (CS1) (5'-ACACTGACGACATGGTTCTACA-3') and  
252 common sequence 2 (CS2) (5'-TACGGTAGCAGAGACTTGGTCT-3') universal primer sequences, required  
253 for Illumina MiSeq amplicon tagging and indexing, were added to the 5' ends of forward and reverse  
254 primers, respectively. Reaction conditions were 98°C for three minutes, followed by 30 cycles of 98°C for  
255 10 seconds, 62°C for 20 seconds and 72°C for 30 seconds. Then a final elongation step of 72°C for 2  
256 minutes was conducted. The first PCR products were used as templates for the second PCR. The second

257 PCR conducted in order to add adapters and tags, as well as the amplified sequences purification were  
258 made by G enome Qu ebec inc.

## 259 **Statistical analysis**

260 Bacterial population analysis results were interpreted using MicrobiomeAnalyst software (Dhariwal,  
261 Chong et al. 2017). The Marker Data Profiling module was used to compare the bacterial population in  
262 the samples taken at different charge loading.

### 263 *2.4.2. Physico-chemical parameters analysis*

264 Water samples (feed and permeate) were analyzed for pH (Mettler Toledo SevenEasy), electrical  
265 conductivity (Mettler Toledo SevenCompact Conductivity), alkalinity (bromocresol green titration), solid  
266 content (total, dissolved, and volatile) (EPA Method 160.2), chemical oxygen demand (CEAEQ MA. 315 –  
267 DCO 1.1, Potassium dichromate), biological oxygen demand (5 days) (CEAEQ MA. 315 – DBO 1.1.),  
268 dissolved ammoniacal nitrogen (QuickChem Method 10-107-06-2-O, salicylate – nitroprusside  
269 colorimetric method), total organic carbon and total nitrogen (Shimadzu VCPH), and total phosphorus  
270 (Varian Vista AX ICP-AES). Total phosphorus content was determined after preliminary sample digestion  
271 (15% trace metals grade HNO<sub>3</sub> and 5% H<sub>2</sub>O<sub>2</sub> at 95°C for 2 hours). Mixed liquor samples were analyzed for  
272 solid content (total, dissolved, and volatile) (EPA Method 160.2).

## 273 *3. Results and discussion*

### 274 *3.1. Nitrate reduction hypothesis validation*

275 In order to confirm the hypothesis of an electrochemical cathodic reduction of nitrates into ammonia  
276 nitrogen suggested by Dia et al. (2017), treated leachates from Condition #1 were exposed to charge

277 loading ranging from 200 to 1 000 mAh L<sup>-1</sup> in an electrocoagulation batch reactor (Dia, Drogui et al.  
 278 2017). The leachate's nitrate and ammonia nitrogen concentrations after a 30-minute exposure to  
 279 different current intensities in Figure 4a and Figure 4b, respectively. Figure 4a and Figure 4b show the  
 280 concentrations using both a Ti/Pt cathode and iron anode, and graphite cathode and iron anode.

281 Initial concentrations of nitrate and ammonia nitrogen in the aerobically treated leachates were 128 mg  
 282 NO<sub>3</sub>-N L<sup>-1</sup> and 1.1 mg NH<sub>4</sub>-N L<sup>-1</sup>, respectively. In Figure 4a, results show that nitrate concentrations  
 283 linearly decreased at a rate of -0.03 mg NO<sub>3</sub>-N mA<sup>-1</sup> h<sup>-1</sup> when a graphite cathode was used. At this rate,  
 284 the leachate's nitrate concentration was reduced by 32 mg NO<sub>3</sub>-N L<sup>-1</sup> after 30 minutes of exposure to 1  
 285 000 mAh L<sup>-1</sup>. With the Ti/Pt cathode, no significant difference in nitrate concentration was observed at  
 286 charge loading below 750 mAh L<sup>-1</sup>. Leachate exposed to 1 000 mAh L<sup>-1</sup> for 30 minutes using a Ti/PT  
 287 cathode saw its concentration reduced by approximately 5 mg NO<sub>3</sub>-N L<sup>-1</sup>, which is 85% less than with the  
 288 graphite electrode at the same charge loading. In Figure 4b, results show that the leachate's ammonia  
 289 nitrogen concentration increased proportionally to the applied charge loading when using the graphite  
 290 cathode. More precisely, the ammonia nitrogen increased from 1.1 to 25 mg NH<sub>4</sub>-N L<sup>-1</sup> after 30 minutes  
 291 with a charge loading of 1 000 mAh L<sup>-1</sup>. This ammonia nitrogen concentration is in accordance with its  
 292 associated nitrate concentration drop (32 mg NO<sub>3</sub>-N L<sup>-1</sup>). With the use of a Ti/Pt cathode, the ammonia  
 293 nitrogen only increased from 1.1 to 1.3 mg NH<sub>4</sub>-N L<sup>-1</sup> after 30 minutes of exposure to a charge loading of  
 294 1 000 mAh L<sup>-1</sup>.

295 According to the results presented in Figure 4a, the rate at which the nitrates are reduced into ammonia  
 296 during the electrocoagulation process depends on the cathode material properties and also is directly  
 297 correlated to the charge loading at high nitrate concentrations. This rate is expressed by Eq. 2.

$$r_{NO_3,EC} = -k_i \frac{I}{V} = -r_{NH_4,EC} \quad \text{Eq. 2}$$

298 Where  $k_i$  is the cathode material's ( $i$ ) nitrate mass reduction rate ( $\text{mg NO}_3\text{-N mA}^{-1} \text{h}^{-1}$ ),  $I$  is the current  
 299 intensity (A), and  $V$  is the reactor's volume (L). These results confirm the Dia et al. (2017) hypothesis that  
 300 a Ti/Pt cathode is a well-suited cathode material for an EC process combined with a bioprocess treating  
 301 ammonia nitrogen, due to its low electrochemical nitrate reduction rate (Dia, Drogui et al. 2017). In an  
 302 Electro-MBR, the steady-state ammonia nitrogen removal is expressed by Eq. 3 (adapted from Roy et al.  
 303 (2020) to include the effect of the EC process (Roy, Drogui et al. 2020)).

$$\frac{(S_{\text{NH}_4,f} - S_{\text{NH}_4,p})}{\text{HRT}} - r_{\text{NH}_4,\text{EC}} = r_{\text{NH}_4,\text{Bio}} * \left(1 - \frac{S_{\text{Alk},p}^*}{S_{\text{Alk},p}}\right)^n \quad \text{Eq. 3}$$

304 According to Eq. 2, ammonia nitrogen removal objectives are obtained when the biological nitrification  
 305 rate ( $r_{\text{NH}_4,\text{Bio}}$ ) is higher than the ammonia load rate combined with the nitrate reduction rate minus the  
 306 maximum allowed ammonia exit rate. Thus, Electro-MBRs' reduced nitrification rates reported in the  
 307 literature could be the result of the use of high HOP cathode materials and high charge loading, both of  
 308 which increase the nitrate reduction rate. To further support this hypothesis, reported effects of electro-  
 309 coagulation systems on Electro-MBR performances in treating ammonia nitrogen from wastewater are  
 310 summarized in Table 3.

311 In both cases where the electrocoagulation was reported to have a negative impact on nitrification  
 312 performances, ammonia loading rates were low ( $36 \text{ mg NH}_4\text{-N L}^{-1} \text{d}^{-1}$  in the synthetic municipal  
 313 wastewater and  $13.6 \text{ mg NH}_4\text{-N L}^{-1} \text{d}^{-1}$  in the grey water) and the charge loading were above  $100 \text{ mAh L}^{-1}$ .  
 314 Considering that the maximum biological nitrification rate ( $r_{\text{NH}_4,\text{Bio}}$ ) value is equal to the ammonia load  
 315 rate when no EC process is used, ammonia obtained from cathodic reduction at the aforementioned  
 316 charge loading after the addition of an EC process will most probably not be removed. This sudden  
 317 excess in ammonia nitrogen can thus significantly impact the reported ammonia removal percentage,  
 318 especially when using cathode materials with high HOP values (Al and Fe).

319 Positive effects were reported at charge loading lower than 144 mAh L<sup>-1</sup>, indicating that the ammonia  
320 oxidizing bacteria can adapt their rate of biological nitrification to the small excess of ammonia nitrogen  
321 generated on the cathode in the EC system. Based on a reaction engineering approach, the increased  
322 *Nitrosomonas* relative abundance reported by Li, Dong et al. (2018) is likely to be the result of an  
323 increased substrate concentration (ammonia nitrogen) resulting from the cathodic reduction of their  
324 product (nitrates). Furthermore, as suggested by Battistelli, da Costa et al. (2018) and Li, Dong et al.  
325 (2018), electrostimulation of both the proton transfer and enzyme activity can improve microbial  
326 metabolism and increase cell growth (Battistelli, da Costa et al. 2018, Li, Dong et al. 2018).

### 327 **3.2. Anodic dissolution rate and coagulant dosage**

328 The anodic dissolution rate governs the charge loading to be applied in order to reach the desired  
329 coagulant concentrations in the mixed liquor. The anodic dissolution rate can be theoretically estimated  
330 using Faraday's law (Eq. 4) (Li, Dong et al. 2018).

$$\dot{m} = \frac{M}{Fn} I \quad \text{Eq. 4}$$

331 Where  $\dot{m}$  is the anodic dissolution rate (g s<sup>-1</sup>),  $M$  is the molar mass of the anode material (g mol<sup>-1</sup>),  $I$  is  
332 the applied current (A),  $F$  is Faraday's constant (96.5 C mol<sup>-1</sup>), and  $n$  is the valence of the anode material.  
333 In order to estimate the anodic dissolution rate of iron anodes in a leachate treating Electro-MBR,  
334 experiments were conducted in the batch reactor at 0.2A with both a NaCl solution with a similar  
335 conductivity as composting leachate (0.2A – Synthetic), as well as real composting leachates (0.2A –  
336 Leachate). Figure 5 compares the experimental results to the theoretical dissolution rate calculated with  
337 Faraday's law.

338 According to Faraday's law, an iron anode should dissolve in the form of ionic three-valent iron at a rate  
339 of 0.7 mg Fe<sup>3+</sup> mAh<sup>-1</sup>. When conducting the anodic dissolution experiment with real leachates, the

340 measured rate was  $0.82 \pm 0.05 \text{ mg Fe}^{3+} \text{ mAh}^{-1}$  (obtained from a duplicate), which is consistent with the  
 341 expected theoretical rate. Iron dosages for Condition #2 ( $100 \text{ mAh L}^{-1}$ ), #3 ( $200 \text{ mAh L}^{-1}$ ), and #4 ( $400$   
 342  $\text{mAh L}^{-1}$ ) were estimated to be 82, 165, and 325  $\text{mg Fe}^{3+} \text{ L}^{-1}$ , respectively, using the following equation  
 343 (Eq. 5):

$$Fe = \dot{m} * \frac{I}{V} * HRT \quad \text{Eq. 5}$$

344 **3.3. Where  $Fe$  is the iron dosage from anodic dissolution ( $\text{mg Fe}^{3+} \text{ L}^{-1}$ ) Effect of**  
 345 ***the charge loading on leachate contaminant removal***

### 346 **3.3.1. Nitrification process performance**

347 MBRs' nitrification performances were reported to be either positively or negatively affected by the  
 348 addition of a submerged EC process inside its mixed liquor. The discussion in Section 3.1. showed that  
 349 negative impacts of the EC process were potentially attributed to the selection of the cathode material.  
 350 With high HOP material, the cathodic nitrate reduction rate pushes the equilibrium toward higher  
 351 concentrations of ammonia nitrogen in the reactor, leading to lower nitrification performances. Ti/Pt  
 352 cathodes were found to have an electrochemical nitrate reduction rate of more than 85% lower than  
 353 conventional cathode materials used in EC processes (Al, Fe and stainless steel) (Dia, Drogui et al. 2017).  
 354 Results in Figure 4b showed that no significant quantities of ammonia nitrogen are produced from  
 355 nitrate cathodic reduction when exposed to charge loading ranging from 200 to 1 000  $\text{mAh L}^{-1}$  when a  
 356 Ti/Pt cathode is used. Thus, by using a Ti/Pt cathode in an Electro-MBR, it was possible to measure the  
 357 effect of different DC charge loading, as well as the iron concentration on the Electro-MBR's nitrification  
 358 performances, by avoiding nitrate reduction. Table 4 presents the nitrogen load rates (NLR) and removal  
 359 percentage for the Electro-MBR operated under charge loading ranging from 0 to 400  $\text{mAh L}^{-1}$

360 (Coagulant dosage ranging from 82 to 325 mg Fe<sup>3+</sup> L<sup>-1</sup>). The high NLR measured at Condition #3 (200  
361 mAh L<sup>-1</sup>) is the result of a HRT change from 24h to 12h, which was done in order to assess the effect of  
362 doubling the NLR on the Electro-MBR's capacity to remove ammonia nitrogen.

363 Interestingly, the ammonia nitrogen removal percentage remained at >99.7% in all conditions with  
364 permeate concentrations ranging from 0.18 to 0.43 mg NH<sub>4</sub>-N L<sup>-1</sup>, which indicate no inhibitory effect of  
365 the charge loading or the iron concentration on the nitrification performance. Removal rates of 119 to  
366 125 mg NH<sub>4</sub>-N L<sup>-1</sup> d<sup>-1</sup> and 243 NH<sub>4</sub>-N L<sup>-1</sup> d<sup>-1</sup> were measured at HRTs of 24h and 12h, respectively. A  
367 previous study on the performance of a MBR treating composting leachate reported similar removal  
368 percentages and rates reaching up to 740 mg NH<sub>4</sub>-N L<sup>-1</sup> d<sup>-1</sup>, indicating no negative impact of the  
369 electrocoagulation on the MBR process (Roy, Drogui et al. 2020). Furthermore, the change in rates  
370 when the HRT was decreased from 24h to 12h indicates that the amoA gene expressing bacteria from  
371 the mixed liquor can quickly adapt to variable ammonia load rates and therefore maintain an almost  
372 complete ammonia removal without inhibition from the application of a charge loading up to 400 mAh L<sup>-1</sup>.  
373 <sup>1</sup>.

374 The nitrification performances of a biological system also depend on the buffering capacity of the  
375 wastewater to be treated. According to the stoichiometry of the nitrification reaction, 7.14 mg of  
376 alkalinity (as CaCO<sub>3</sub>) is consumed for every milligram of ammonia nitrogen oxidized to nitrate (Roy,  
377 Benkaraache et al. 2019). If this ratio is not maintained, a pH drop will occur and nitrification will be  
378 inhibited (Lee, Kim et al. 2001). Roy et al. (2020) reported that a residual concentration of 200 mg  
379 CaCO<sub>3</sub> L<sup>-1</sup> is required to maintain high nitrification performances (Roy, Drogui et al. 2020). Therefore,  
380 alkalinity consumption was monitored at each tested condition. Both feed and permeate concentrations  
381 are presented in Table 4. Without applied current, the measured alkalinity consumption was 7.51 mg  
382 CaCO<sub>3</sub> per 1 mg NH<sub>4</sub>-N L<sup>-1</sup> and was entirely attributed to biological nitrification. This ratio was assumed  
383 to be constant for all other conditions, and any consumed excess alkalinity was attributed to the EC

384 process. The EC process's alkalinity consumption increased from 8 mg CaCO<sub>3</sub> L<sup>-1</sup> to 269 mg CaCO<sub>3</sub> L<sup>-1</sup>  
385 when the applied charge loading increased from 100 to 400 mAh L<sup>-1</sup>. At 400 mAh L<sup>-1</sup>, permeate's Ca<sup>2+</sup>  
386 concentration decreased from 178.1 to 78.6 mg Ca<sup>2+</sup> L<sup>-1</sup>, which is almost equimolar to the loss in  
387 alkalinity (0.93 mol Ca<sup>2+</sup>:mol CaCO<sub>3</sub>). This alkalinity consumption thus results from the formation of a  
388 CaCO<sub>3</sub> precipitate on the cathode surface where highly alkaline conditions are created by the release of  
389 OH<sup>-</sup>. Therefore, EC can consume alkalinity if no current inversion is done in order to dissolved the CaCO<sub>3</sub>  
390 precipitate on the cathode surface (Zhu, Clifford et al. 2005). Therefore, if the alkalinity in the  
391 wastewater is not sufficient to account for both the biological and the EC consumption, this parameter  
392 can also lead to lower nitrification performances in Electro-MBRs.

### 393 ***3.3.2. Total organic carbon and total phosphorus removal performances***

394 Table 5 presents the feed and permeate TOC and dissolved iron concentrations from the Electro-MBR  
395 when treating co-composting leachates operated with charge loading ranging from 0 to 400 mAh L<sup>-1</sup>.

396 When operated without applied current, the MBR achieved a mere 13% removal in TOC, indicating that  
397 the recalcitrant fraction of TOC represents 87% of the organic contamination. The electrochemical  
398 dosage of ferric ions at concentrations of 82 to 325 mg Fe<sup>3+</sup> L<sup>-1</sup> (corresponding to charge loading of 100  
399 to 400 mAh L<sup>-1</sup>) then increased the TOC removal from 25 to 38%, respectively. These results are in  
400 accordance with those of Maleki and al. (2009) which reported COD removal percentages of 28% from  
401 composting leachate at an iron dosage of 680 mg Fe L<sup>-1</sup> using iron salts as coagulating agents (Maleki,  
402 Zazouli et al. 2009, Mahvi, feizabadi et al. 2015). Lower dissolved iron concentrations measured in the  
403 permeate when compared to the feed indicate that all the iron released from the sacrificial anode was  
404 precipitated with the biomass and remained in the mixed liquor.

405 In order to assess the efficiency of the ferric ions in coagulating the leachate's TOC in an Electro-MBR, a  
406 mass balance between the amount of ferric ions generated and the TOC removed was conducted. Figure

407 6a distinguishes the biologically oxidized TOC from the chemically precipitated TOC, while Figure 6b  
408 presents the ratios of TOC coagulated per mass of ferric iron generated in the mixed liquor at charge  
409 loading from 100 to 400 mAh L<sup>-1</sup>.

410 According to the results shown in Figure 6a, the MBR removed 35 mg TOC L<sup>-1</sup> when operated without  
411 applied current at a HRT of 24h and a SRT of 45 days. Then, at Conditions #2, #3, and #4, all the TOC that  
412 was removed beyond the aforementioned concentration was assumed to be physico-chemically  
413 precipitated by the EC process. The most TOC removal was obtained at 400 mAh L<sup>-1</sup>, with a total of 67  
414 mg TOC L<sup>-1</sup>. However, in terms of efficiency, the highest ratio of TOC:Fe<sup>3+</sup> was obtained at 100 mAh L<sup>-1</sup>,  
415 with a value of 0.44 ± 0.5 mg TOC mg Fe<sup>-1</sup>. For charge loading of 200 to 400 mAh L<sup>-1</sup>, the TOC:Fe<sup>3+</sup>  
416 efficiency reached a plateau at 0.19 ± 0.2 mg TOC mg Fe<sup>-1</sup>. These results are in accordance with those  
417 from Amokrane et al. (1995) (Amokrane, Comel et al. 1997). At low iron concentrations (<200 mg L<sup>-1</sup>),  
418 highly charged organic molecules react quickly with ferric ions and then precipitate. The TOC:Fe<sup>3+</sup> ratio  
419 then remains constant (removal percentage is proportional to the ferric iron dosage) until most organic  
420 molecules with polar moieties have precipitated.

421 The Electro-MBR efficiency in removing phosphorus from leachate was also assessed by conducting a  
422 mass balance between the quantity of generated ferric ions and the precipitated total phosphorus (P<sub>tot</sub>).  
423 Table 6 presents the feed and permeate P<sub>tot</sub> concentrations, as well as the P<sub>tot</sub>:Fe<sup>3+</sup> ratio, for the Electro-  
424 MBR treating co-composting leachates and operated under charge loading ranging from 0 to 400 mAh L<sup>-1</sup>  
425 <sup>1</sup>.

426 P<sub>tot</sub> removal percentages are positively correlated with the iron dosage, which is in accordance with  
427 previous studies on Electro-MBRs (Bani-Melhem and Smith 2012, Tian, He et al. 2016). As opposed to  
428 the TOC, P<sub>tot</sub> removal efficiency was at its highest at 400 mAh L<sup>-1</sup> with a P<sub>tot</sub>:Fe<sup>3+</sup> ratio of 60 mg P<sub>tot</sub> g Fe<sup>-1</sup>.  
429 The increased P<sub>tot</sub> removal efficiency at higher ferric ion concentrations is linked to the TOC removal. At

430 low  $\text{Fe}^{3+}$  concentrations, all the coagulant is scavenged by the highly charged TOC. Then, at higher  $\text{Fe}^{3+}$   
431 concentrations, more coagulant remains available for the  $P_{\text{tot}}$  to react with, leading to higher  $P_{\text{tot}}:\text{Fe}^{3+}$   
432 ratios.

### 433 *3.4. Effect of the charge loading on the mixed liquor microbial population*

#### 434 *diversity and structure*

435 In the previous sections, it was demonstrated that lower nitrification performances, rather than being  
436 related to inhibition phenomena, were instead potentially related to the magnitude of the cathode  
437 material's nitrate electrochemical reduction rate and to a possible lack of buffering capacity (alkalinity)  
438 in the wastewater. To further support this statement, changes in microbial population diversity and  
439 structure were monitored at each tested condition. The  $\alpha$ -diversity (Chao1), as well as the rarefaction  
440 curves, are presented in Figure 7a and Figure 7b, respectively. The Chao1 method was selected in order  
441 to estimate the number of unique species while accounting for low-abundance operational taxonomic  
442 units (OTUs) (Dhariwal, Chong et al. 2017).

443 The Chao1  $\alpha$ -diversity analysis conducted on both the MBR's and the Electro-MBR's mixed liquors  
444 showed a stable diversity in the microbial community ( $\alpha$ -diversity =  $169 \pm 3$ ), except at Condition #3 ( $\alpha$ -  
445 diversity = 140), where the Electro-MBR was operated at a HRT of 12h instead of 24h. In terms of  
446 species richness analysis, Condition #3 also resulted in the lowest number of OTUs, with 1 980 OTUs.  
447 The number of OTUs in the other samples ranged from 2 120 to 2 425, with the sample that was  
448 exposed to a charge loading of  $400 \text{ mAh L}^{-1}$  having the highest count. The similarities in  $\alpha$ -diversity and  
449 species richness between the mixed liquor samples collected from both the MBR and the Electro-MBR  
450 when operated at a HRT of 24h, indicate that both charge loading that range from 100 to  $400 \text{ mAh L}^{-1}$ , as  
451 well as the associated ferric ions concentrations, both have no significant impact on the diversity of  
452 microbial genus in mixed liquor. Furthermore, the significantly lower  $\alpha$ -diversity measured at a HRT of

453 12h indicates that the contaminant load rate has more impact on the community diversity than the  
454 charge loading applied would.

455 Both the MBR's and the Electro-MBR's microbial population structure at the genus level is presented in  
456 Figure 8. No dominant OTU genus (relative abundance >10%) was detected in the MBR's mixed liquor  
457 without applied current. Instead, the population contained three sub-dominant OTU genera (relative  
458 abundance >3%) that were: *Reyranella* (7.8%), *Trichococcus* (5.1%), and *Nitrosomonas* (4.8%). Both  
459 *Reyranella* and *Trichococcus* are heterotrophic bacteria ubiquitous to biological wastewater treatment  
460 processes. *Trichococcus* are filamentous bacteria commonly found in bulking sludge (Scheff, Salcher et  
461 al. 1984). Vandewalle et al. (2012) also reported this genus to be dominant in urban sewer infrastructure  
462 (Vandewalle, Goetz et al. 2012). After the addition of the EC system with a HRT of 24h (Condition #2 and  
463 #4), *Reyranella* and *Nitrosomonas* remained subdominant genera, while *Trichococcus* became a  
464 dominant genus. At charge loading of 100 and 400 mAh L<sup>-1</sup>, the dominant and sub-dominant genera's  
465 relative abundance were: 10.3% and 12.7% for *Trichococcus*, 8.7% and 4.3% for *Reyranella*, and 5.6%  
466 and 8.2% for *Nitrosomonas*. These results indicate that the presence of coagulant might have favoured  
467 the development of floc-forming bacteria, which could be related to the lower membrane fouling  
468 propensity in Electro-MBRs (Borea, Naddeo et al. 2017). Another interesting observation is the positive  
469 correlation between the *Nitrosomonas*, the main ammonia nitrogen oxidizing bacteria identified in the  
470 mixed liquor, and the charge loading. Compared to the MBR without applied current, *Nitrosomonas*  
471 relative abundance almost doubled when exposed to a charge loading of 400 mAh L<sup>-1</sup>, increasing from  
472 4.8% to 8.2%. This result supports the findings of Li et al. (2018), which reported an increase in  
473 *Nitrosomonas* relative abundance of 1.45% to 3.12% when exposed to a charge loading of 14 mAh L<sup>-1</sup> in  
474 the study's Electro-MBR treating a synthetic wastewater (40 mg NH<sub>4</sub>-N L<sup>-1</sup>) (Li, Dong et al. 2018). The  
475 effect of the electrocoagulation system is explained by two elements; first, since a microbial population  
476 size is generally proportional to the amount of substrate available, the increased amount of substrate

477 (ammonia nitrogen) from nitrate cathodic reduction is likely to result in a larger population of  
478 *Nitrosomonas*. Second, as previously reported by Qian et al. (2017), the use of EC integrated in  
479 bioreactors can improve the biomass enzymatic activity of nitrifying bacteria, mainly the ammonia  
480 monooxygenase (AMO), hydroxylamine oxidoreductase (HAO), and nitrite oxidoreductase (NOR), which  
481 would result in increased nitrifying bacteria growth (Qian, Hu et al. 2017). In terms of contaminant load  
482 rate, the change in HRT had a significant impact on the microbial population structure. At a HRT of 12h  
483 (Condition #3), *Trichococcus* genus increased its relative abundance to 20.2%, and several subdominant  
484 genera also appeared, including: *Nitrobacter* (5.4%), *Chryseobacterium* (4.1%), *Pirellula* (4.1%),  
485 *Proteiniclasticum* (3.3%), and *Paludibaculum* (3.0%). In a previous study on MBR treating composting  
486 leachates, all these subdominant genera, with the exception of *Chryseobacterium*, were identified at a  
487 SRT of 45 days under similar contaminant load rates. *Nitrobacter* was also reported in higher  
488 abundances at low HRT (Roy et al. 2020). Interestingly, at a HRT of 12h, *Nitrosomonas* relative  
489 abundance decreased to only 0.8% while the NLR increased from 124 to 244 mg NH<sub>4</sub>-N L<sup>-1</sup> d<sup>-1</sup>. Despite a  
490 lower *Nitrosomonas* relative abundance when compared to the other conditions, the ammonia nitrogen  
491 removal percentage at Condition #3 remained above 99.7%. These results are in accordance with those  
492 of Roy et al. (2020), which reported that *Nitrosomonas* growth is inhibited in a MBR by increasing the  
493 organic load rate (OLR), yet nitrification performances are unaffected by the OLR and the *Nitrosomonas*  
494 relative abundance.

495 Results from the microbial community structure and diversity analyses indicate that neither charge  
496 loading ranging from 100 to 400 mAh L<sup>-1</sup> nor their associated ferric iron concentrations have any  
497 inhibitive impact on *Nitrosomonas* growth. Rather, *Nitrosomonas* growth is positively correlated to the  
498 applied charge loading under these conditions. The HRT was found to have significantly more impact on  
499 the microbial population structure than the DC current. Thus, lower nitrification performances are  
500 expected in studies where membrane fouling is compensated by constantly varying the HRT (ex.: Bani-

501 Melhem and Smith (2012) (Bani-Melhem and Smith 2012)), whereas higher performances are expected  
502 when the membrane is instead changed or frequently cleaned. As opposed to the hypothesis made from  
503 the authors of these studies, these lower performances are the result of a constant adaptation of the  
504 mixed liquor to the contaminant load rates, as well as a loss in *Nitrosomonas* population, and are not  
505 related to the applied current.

#### 506 **4. Conclusion**

507 In this study, Electro-MBR technology was evaluated for the treatment of high-strength ammonia  
508 wastewater with an initial ammonia nitrogen concentration of  $124 \pm 4$  mg  $\text{NH}_4\text{-N L}^{-1}$ . Using a  
509 combination of a sacrificial iron anode and a Ti/Pt cathode, as well as a charge loading of  $400 \text{ mAh L}^{-1}$ ,  
510 removal percentages of 99.8%, 38%, and 99.0% of ammonia nitrogen, TOC, and  $\text{P}_{\text{tot}}$ , respectively, were  
511 obtained. This configuration of Electro-MBR is thus promising in solving the challenges associated with  
512 the treatment of waste originating leachates.

513 This study's second objective was to shed light on reported divergent impacts on nitrification  
514 performances when an EC process was added to an MBR. First, the effect of the cathode material on the  
515 cathodic nitrate reduction rate was evaluated. Results showed that high HOP cathode materials, such as  
516 graphite, reduce nitrate to ammonia nitrogen at a rate that outpaces the biological nitrification rate. The  
517 solution to overcome this issue is to use low HOP cathode material such as Ti/Pt, which favours water  
518 reduction to hydrogen. Then, the effect of the charge loading the nitrification performances was  
519 assessed. No significant impact was observed on the nitrification performances when using a Ti/Pt  
520 cathode with charge loading ranging from 100 to  $400 \text{ mAh L}^{-1}$ . These charge loading had also no  
521 significant impact on the microbial community diversity, while a lower HRT resulted in a lower OTUs  
522 count. In terms of community structure, *Nitrosomonas* relative abundance increased proportionally with

523 the charge loading, showing no inhibitive phenomena due to the iron concentration or the applied DC  
524 current. In general, high nitrification rates in Electro-MBR can be obtained when using a Ti/Pt cathode.

### 525 *Acknowledgements*

526 Support for this study was provided by the NSERC, under a cooperative agreement with the Institut  
527 national de la recherche scientifique (INRS), Englobe Corp., and Centre National en Électrochimie et en  
528 Technologies Environnementales (CNETE); and by a MITACS doctoral scholarship from MITACS and  
529 Englobe Corp. The author would also like to thank Nathalie Couët for copy editing.

530

531

532 *References*

- 533 Amokrane, A., C. Comel and J. Veron (1997). "Landfill leachates pretreatment by coagulation-  
534 flocculation." Water Research **31**(11): 2775-2782.
- 535 Bani-Melhem, K. and M. Elektorowicz (2010). "Development of a novel submerged membrane electro-  
536 bioreactor (SMEBR): performance for fouling reduction." Environmental science & technology **44**(9):  
537 3298-3304.
- 538 Bani-Melhem, K. and M. Elektorowicz (2011). "Performance of the submerged membrane electro-  
539 bioreactor (SMEBR) with iron electrodes for wastewater treatment and fouling reduction." Journal of  
540 Membrane Science **379**(1): 434-439.
- 541 Bani-Melhem, K. and E. Smith (2012). "Grey water treatment by a continuous process of an  
542 electrocoagulation unit and a submerged membrane bioreactor system." Chemical Engineering Journal  
543 **198**: 201-210.
- 544 Battistelli, A., T. Belli, R. Costa, N. Justino, D. Silveira, M. Lobo-Recio and F. Lapolli (2019). "Application of  
545 low-density electric current to performance improvement of membrane bioreactor treating raw  
546 municipal wastewater." International Journal of Environmental Science and Technology **16**(8): 3949-  
547 3960.
- 548 Battistelli, A. A., R. E. da Costa, L. Dalri-Cecato, T. J. Belli and F. R. Lapolli (2018). "Effects of  
549 electrochemical processes application on the modification of mixed liquor characteristics of an electro-  
550 membrane bioreactor (e-MBR)." Water Science and Technology **78**(11): 2364-2373.
- 551 Borea, L., V. Naddeo and V. Belgiorno (2017). "Application of electrochemical processes to membrane  
552 bioreactors for improving nutrient removal and fouling control." Environmental Science and Pollution  
553 Research **24**(1): 321-333.
- 554 Canziani, R., V. Emondi, M. Garavaglia, F. Malpei, E. Pasinetti and G. Buttiglieri (2006). "Effect of oxygen  
555 concentration on biological nitrification and microbial kinetics in a cross-flow membrane bioreactor

- 556 (MBR) and moving-bed biofilm reactor (MBBR) treating old landfill leachate." Journal of Membrane  
557 Science **286**(1): 202-212.
- 558 Dhariwal, A., J. Chong, S. Habib, I. L. King, L. B. Agellon and J. Xia (2017). "MicrobiomeAnalyst: a web-  
559 based tool for comprehensive statistical, visual and meta-analysis of microbiome data." Nucleic Acids  
560 Research **45**(W1): W180-W188.
- 561 Dia, O., P. Drogui, G. Buelna and R. Dubé (2017). "Strategical approach to prevent ammonia formation  
562 during electrocoagulation of landfill leachate obtained from a biofiltration process." Separation and  
563 Purification Technology **189**: 253-259.
- 564 Ensano, B. M. B., L. Borea, V. Naddeo, V. Belgiorno, M. D. G. de Luna and F. C. Ballesteros (2016).  
565 "Combination of Electrochemical Processes with Membrane Bioreactors for Wastewater Treatment and  
566 Fouling Control: A Review." Frontiers in Environmental Science **4**(57).
- 567 Gagnaire, J., X. Y. Wang, L. Chapon, P. Moulin and B. Marrot (2011). "Kinetic study of compost liquor  
568 nitrification." Water Sci Technol **63**(5): 868-876.
- 569 He, S.-b., G. Xue and B.-z. Wang (2009). "Factors affecting simultaneous nitrification and de-nitrification  
570 (SND) and its kinetics model in membrane bioreactor." Journal of Hazardous Materials **168**(2): 704-710.
- 571 Herlemann, D. P., M. Labrenz, K. Jurgens, S. Bertilsson, J. J. Waniek and A. F. Andersson (2011).  
572 "Transitions in bacterial communities along the 2000 km salinity gradient of the Baltic Sea." Isme j **5**(10):  
573 1571-1579.
- 574 Kim, H.-G., H.-N. Jang, H.-M. Kim, D.-S. Lee and T.-H. Chung (2010). "Effect of an electro phosphorous  
575 removal process on phosphorous removal and membrane permeability in a pilot-scale MBR."  
576 Desalination **250**(2): 629-633.
- 577 Lee, J. C., J. S. Kim, I. J. Kang, M. H. Cho, P. K. Park and C. H. Lee (2001). "Potential and limitations of alum  
578 or zeolite addition to improve the performance of a submerged membrane bioreactor." Water Science  
579 and Technology **43**(11): 59-66.

- 580 Li, L., Y. Dong, G. Qian, X. Hu and L. Ye (2018). "Performance and microbial community analysis of bio-  
581 electrocoagulation on simultaneous nitrification and denitrification in submerged membrane bioreactor  
582 at limited dissolved oxygen." Bioresource technology **258**: 168-176.
- 583 Li, X.-G., H.-B. Cao, J.-C. Wu and K.-T. Yu (2001). "Inhibition of the metabolism of nitrifying bacteria by  
584 direct electric current." Biotechnology Letters **23**(9): 705-709.
- 585 Mahvi, A. H., G. K. feizabadi, M. H. Dehghani and S. Mazloomi (2015). "Efficiency of different coagulants  
586 in pretreatment of composting plant leachate." Journal of Biodiversity and Environmental Sciences **6**(6):  
587 21-28.
- 588 Maleki, A., M. A. Zazouli, H. Izanloo and R. Rezaee (2009). "Composting plant leachate treatment by  
589 coagulation-flocculation process." American-Eurasian Journal of Agricultural and Environmental Sciences  
590 **5**(5): 638-643.
- 591 Qian, G., X. Hu, L. Li, L. Ye and W. Lv (2017). "Effect of iron ions and electric field on nitrification process  
592 in the periodic reversal bio-electrocoagulation system." Bioresource technology **244**: 382-390.
- 593 Ramirez, E. R. (1976). Electrocoagulation system for removing pollutants from wastewater, Google  
594 Patents.
- 595 Roy, D., A. Azaïs, S. Benkaraache, P. Drogui and R. D. Tyagi (2018). "Composting leachate:  
596 characterization, treatment, and future perspectives." Reviews in Environmental Science and  
597 Bio/Technology **17**(2): 323-349.
- 598 Roy, D., S. Benkaraache, A. Azaïs, P. Drogui and R. D. Tyagi (2019). "Leachate treatment: Assessment of  
599 the systemic changes in the composition and biodegradability of leachates originating in an open co-  
600 composting facility in Canada." Journal of Environmental Chemical Engineering **7**(3): 103056.
- 601 Roy, D., S. Benkaraache, J.-F. Lemay, D. Landry, P. Drogui and R. D. Tyagi (2019). "High-strength  
602 ammonium wastewater treatment by MBR: Steady-state nitrification kinetic parameters." Journal of  
603 Water Process Engineering **32**: 100945.

- 604 Roy, D., P. Drogui, R. D. Tyagi, D. Landry and M. Rahni (2020). "MBR treatment of leachates originating  
605 from waste management facilities: A reference study of the design parameters for efficient treatment."  
606 Journal of Environmental Management **259**: 110057.
- 607 Scheff, G., O. Salcher and F. Lingens (1984). "Trichococcus flocculiformis gen. nov. sp. nov. A new gram-  
608 positive filamentous bacterium isolated from bulking sludge." Applied Microbiology and Biotechnology  
609 **19**(2): 114-119.
- 610 Tafti, A. D., S. M. S. Mirzaii, M. R. Andalibi and M. Vossoughi (2015). "Optimized coupling of an  
611 intermittent DC electric field with a membrane bioreactor for enhanced effluent quality and hindered  
612 membrane fouling." Separation and Purification Technology **152**: 7-13.
- 613 Tian, Y., W. He, X. Zhu, W. Yang, N. Ren and B. E. Logan (2016). "Improved electrocoagulation reactor for  
614 rapid removal of phosphate from wastewater." ACS Sustainable Chemistry & Engineering **5**(1): 67-71.
- 615 Vandewalle, J., G. Goetz, S. Huse, H. Morrison, M. Sogin, R. Hoffmann, K. Yan and S. McLellan (2012).  
616 "Acinetobacter, Aeromonas and Trichococcus populations dominate the microbial community within  
617 urban sewer infrastructure." Environmental microbiology **14**(9): 2538-2552.
- 618 Vuono, D. C., J. Regnery, D. Li, Z. L. Jones, R. W. Holloway and J. r. E. Drewes (2016). "rRNA gene  
619 expression of abundant and rare activated-sludge microorganisms and growth rate induced  
620 micropollutant removal." Environmental science & technology **50**(12): 6299-6309.
- 621 Wei, V., M. Elektorowicz and J. Oleszkiewicz (2012). "Electrically enhanced MBR system for total nutrient  
622 removal in remote northern applications." Water Science and Technology **65**(4): 737-742.
- 623 Wei, V., M. Elektorowicz and J. A. Oleszkiewicz (2011). "Influence of electric current on bacterial viability  
624 in wastewater treatment." Water Research **45**(16): 5058-5062.
- 625 Wei, V., J. Oleszkiewicz and M. Elektorowicz (2009). "Nutrient removal in an electrically enhanced  
626 membrane bioreactor." Water Science and Technology **60**(12): 3159-3163.

- 627 Wei, Y., X. Shi, H. Zhang, J. Wang, B. Zhou and J. Dai (2009). "Combined effects of polyfluorinated and  
628 perfluorinated compounds on primary cultured hepatocytes from rare minnow (*Gobiocypris rarus*) using  
629 toxicogenomic analysis." Aquat Toxicol **95**.
- 630 Wu, J., F. Chen, X. Huang, W. Geng and X. Wen (2006). "Using inorganic coagulants to control membrane  
631 fouling in a submerged membrane bioreactor." Desalination **197**(1-3): 124-136.
- 632 Zhu, B., D. A. Clifford and S. Chellam (2005). "Comparison of electrocoagulation and chemical  
633 coagulation pretreatment for enhanced virus removal using microfiltration membranes." Water  
634 Research **39**(13): 3098-3108.
- 635

Table 1 Operating parameters of the Electro-MBR

Parameters		Condition #1	Condition #2	Condition #3	Condition #4
Period length	(d)	28	14	14	14
Charge loading	(mAh L <sup>-1</sup> )	0	100	200	400
Current density	A m <sup>-2</sup>	0	2.3	4.5	9.1
Temperature	(°C)	20 ± 1	20 ± 1	20 ± 1	20 ± 1
HRT	(hr)	24 ± 2	24 ± 2	12 ± 1	24 ± 2
TSS	(mg L <sup>-1</sup> )	7 800 ± 50	7 870 ± 250	14 340 ± 620	12 660 ± 710
MLVSS	(mg L <sup>-1</sup> )	5 100 ± 50	4 995 ± 170	6 840 ± 260	6 480 ± 570
OLR	(mg COD L <sup>-1</sup> d <sup>-1</sup> )	1100 ± 110	1100 ± 110	1790 ± 180	1100 ± 110
NLR	(mg NH <sub>4</sub> -N L <sup>-1</sup> d <sup>-1</sup> )	125 ± 1	124 ± 2	244 ± 2	119 ± 4
PLR	(mg P L <sup>-1</sup> d <sup>-1</sup> )	4.5 ± 0.2	4.9 ± 0.3	17.4 ± 0.8	9.7 ± 1.2

Table 2 Co-composting leachate characterization

Parameter	Units	Min. - Max. value
Alkalinity	(mg CaCO <sub>3</sub> L <sup>-1</sup> )	1 493 - 1 593
Ammonia nitrogen	(mg NH <sub>4</sub> -N L <sup>-1</sup> )	114 - 129
BOD <sub>5</sub>	(mg L <sup>-1</sup> )	70 - 210
COD	(mg L <sup>-1</sup> )	860 - 1 200
TOC	(mg L <sup>-1</sup> )	244 - 297
Conductivity	(mS cm <sup>-1</sup> )	3.65 - 3.78
Nitrate	(mg NO <sub>3</sub> -N L <sup>-1</sup> )	0.1 - 0.6
pH	-	7.9 - 8.3
Total dissolved solids	(mg L <sup>-1</sup> )	2 190 - 2 820
Total nitrogen	(mg N L <sup>-1</sup> )	129 - 145
Total phosphorus	(mg P L <sup>-1</sup> )	4.3 - 10.7
Total solids	(mg L <sup>-1</sup> )	2 440 - 2 830

Table 3 Reported effects of electro-coagulation systems on Electro-MBR performances in treating ammonia nitrogen

Electrodes material		Charge loading	Wastewater	Effect of Electro-coagulation on nitrification	Authors
Anode	Cathode	(mAh L <sup>-1</sup> )			
Aluminum	Iron	110	Synthetic municipal wastewater	<b>Negative</b> 27% loss in ammonia nitrogen removal	(Bani-Melhem and Elektorowicz 2011)
Aluminum	Aluminum	680	Grey water	<b>Negative</b> 20% loss in ammonia nitrogen removal	(Bani-Melhem and Smith 2012)
Iron	Stainless steel	36 - 165	Synthetic municipal wastewater	<b>Positive</b> Improved nitrification at charge loading <144 mAh L <sup>-1</sup>	(Tafti, Mirzaii et al. 2015)
Aluminum	Stainless steel	15 - 40	Synthetic municipal wastewater	<b>Positive</b> 10.5 to 27% increased in ammonia nitrogen removal	(Borea, Naddeo et al. 2017)
Graphite	Iron	14	Synthetic municipal wastewater	<b>Positive</b> Nitrosomonas relative abundance increase from 1.45 to 3.12%	(Li, Dong et al. 2018)

Table 4 Ti/Pt - Fe Electro-MBR's ammonia nitrogen removal performances and associated alkalinity consumption

Charge loading	Ammonia nitrogen				Alkalinity		
	NLR	Feed	Permeate	Removal	Feed	Permeate	EC consumption
(mAh L <sup>-1</sup> )	(mg NH <sub>4</sub> -N L <sup>-1</sup> d <sup>-1</sup> )	(mg NH <sub>4</sub> -N L <sup>-1</sup> )	(mg NH <sub>4</sub> -N L <sup>-1</sup> )	(%)	(mg CaCO <sub>3</sub> L <sup>-1</sup> )	(mg CaCO <sub>3</sub> L <sup>-1</sup> )	(mg CaCO <sub>3</sub> L <sup>-1</sup> )
0	125	125	0.43	99.7%	1541	598	0
100	124	124	0.34	99.7%	1528	590	8
200	244	122	0.38	99.7%	1563	426	221
400	119	119	0.18	99.8%	1548	383	269

Table 5 Ti/Pt - Fe Electro-MBR's TOC removal performances

Charge loading	Feed		Permeate		TOC Removal
(mAh L <sup>-1</sup> )	(mg TOC L <sup>-1</sup> )	(mg Fe L <sup>-1</sup> )	(mg TOC L <sup>-1</sup> )	(mg Fe L <sup>-1</sup> )	(% TOC)
0	260	3.2	225	0.7	13%
100	280	3.7	211	0.5	25%
200	263	3.2	187	0.3	29%
400	268	4.0	166	0.2	38%

Table 6 Ti/Pt - Fe Electro-MBR's Total phosphorus removal performances

Charge loading	PLR	Feed	Permeate	Removal	$Y_{(P/Fe)}$
(mAh L <sup>-1</sup> )	(mg P L <sup>-1</sup> d <sup>-1</sup> )	(mg P L <sup>-1</sup> )	(mg P L <sup>-1</sup> )	(%)	(mg P:g Fe)
0	4.5	4.5	1.3	71.1%	0
100	4.9	4.9	0.5	89.8%	45.7
200	17.4	8.7	0.3	96.6%	43.4
400	9.7	9.7	0.1	99.0%	60.3

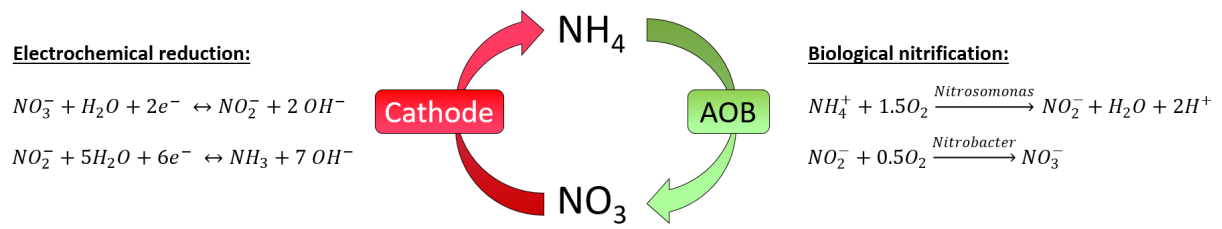
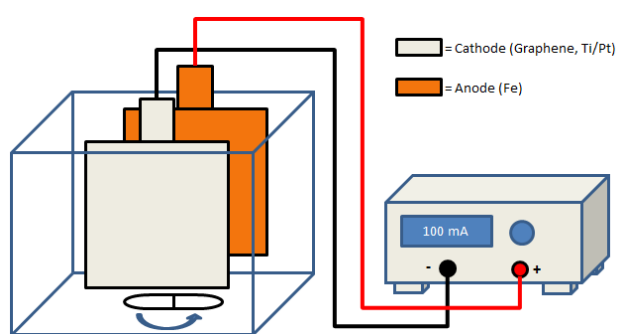
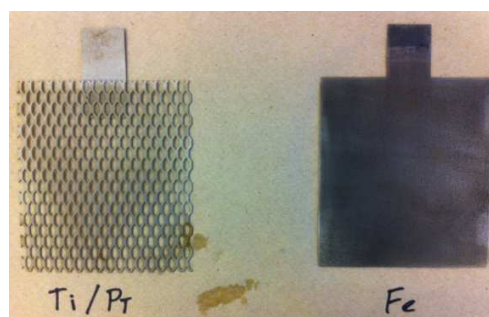


Figure 1 Nitrogen cycle in an aerobic biological / electrochemical combined process

Journal Pre-proof



(a)



(b)

Figure 2 (a) Diagram of the lab-scale electrocoagulation batch reactor, and (b) set of electrodes used in this study

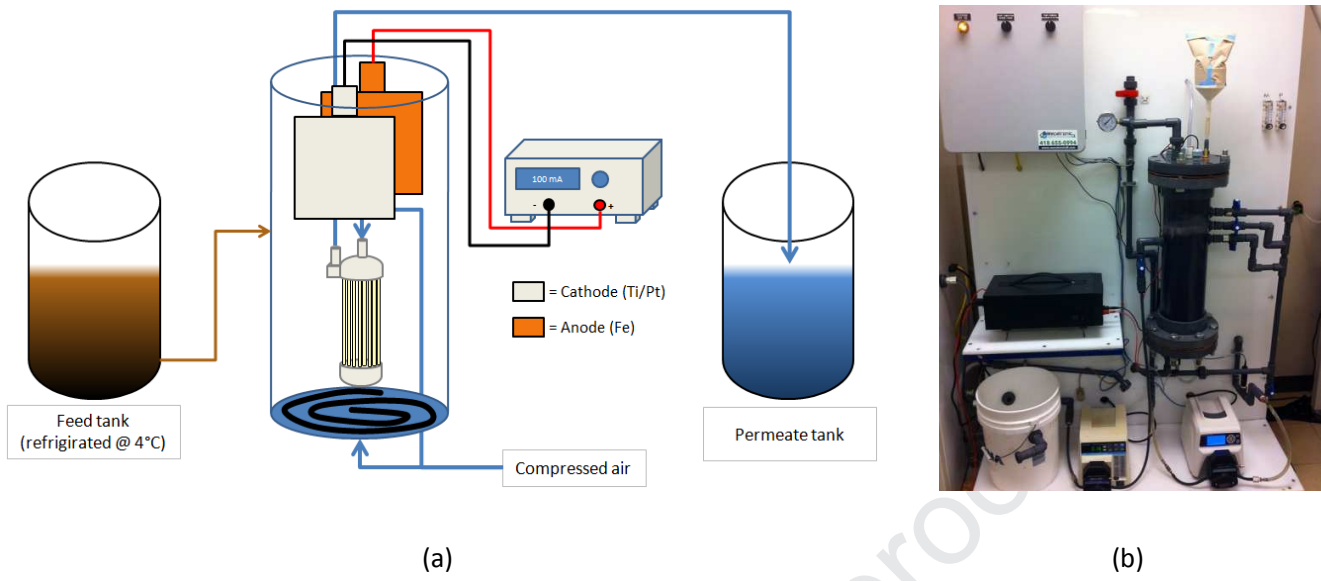
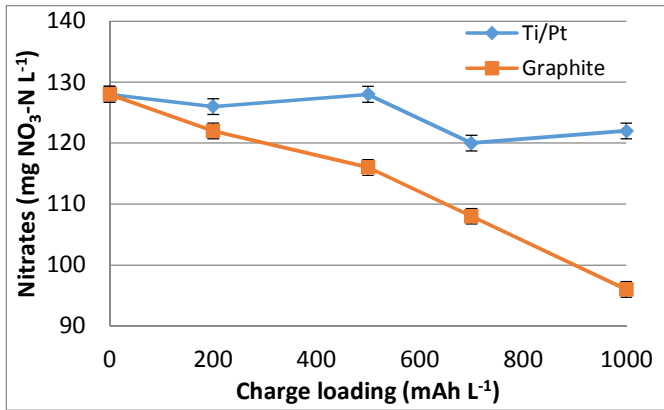
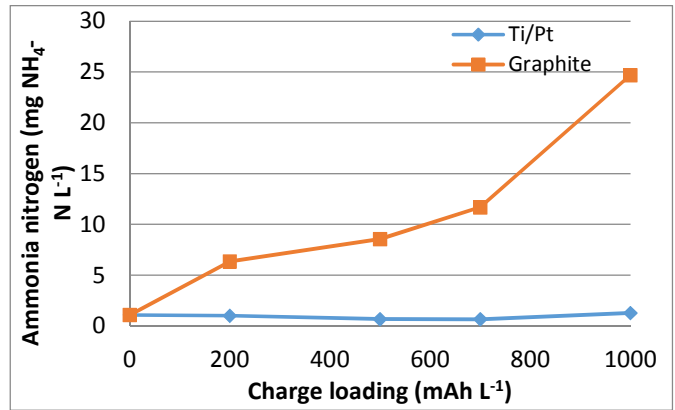


Figure 3 (a) Diagram of the lab-scale submerged membrane bioreactor and (b) Picture of experimental set-up



(a)



(b)

Figure 4 Effect of the charge loading on leachate's a) nitrate concentrations and b) ammonia nitrogen concentration

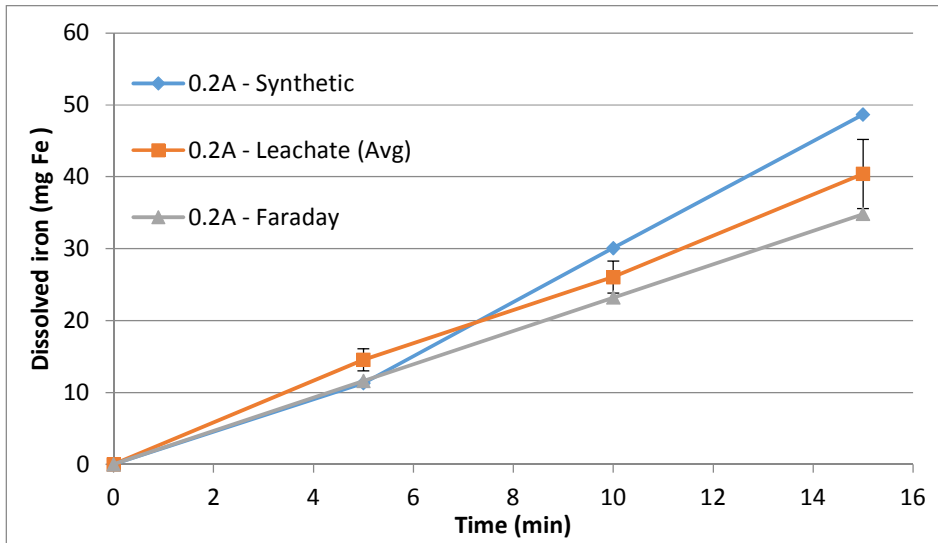
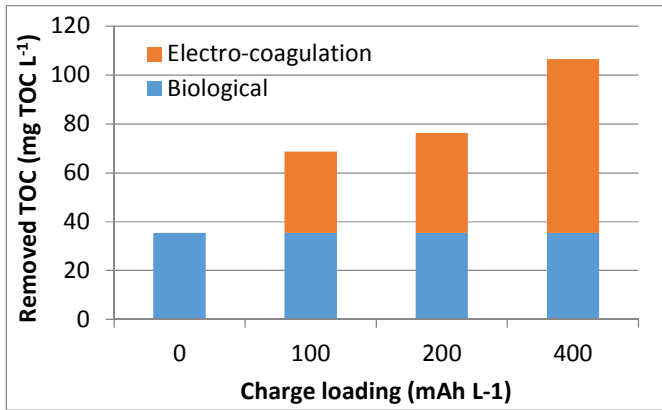
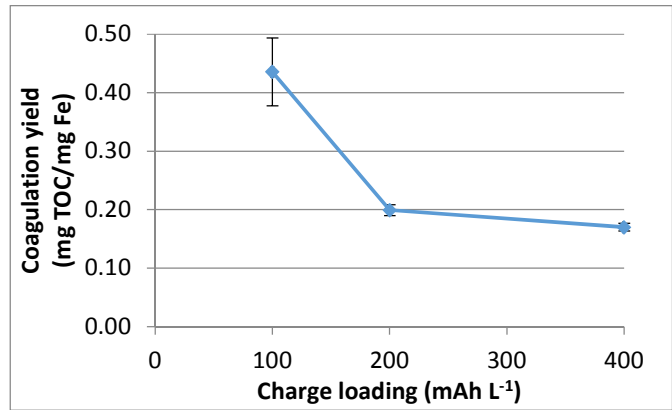


Figure 5 Anodic dissolution rate measurements at a current intensity of 200 mA



(a)



(b)

Figure 6 (a) Biological and physico-chemical fraction of TOC removed by the Electro-MBR and (b) TOC coagulation efficiency at different charge loading

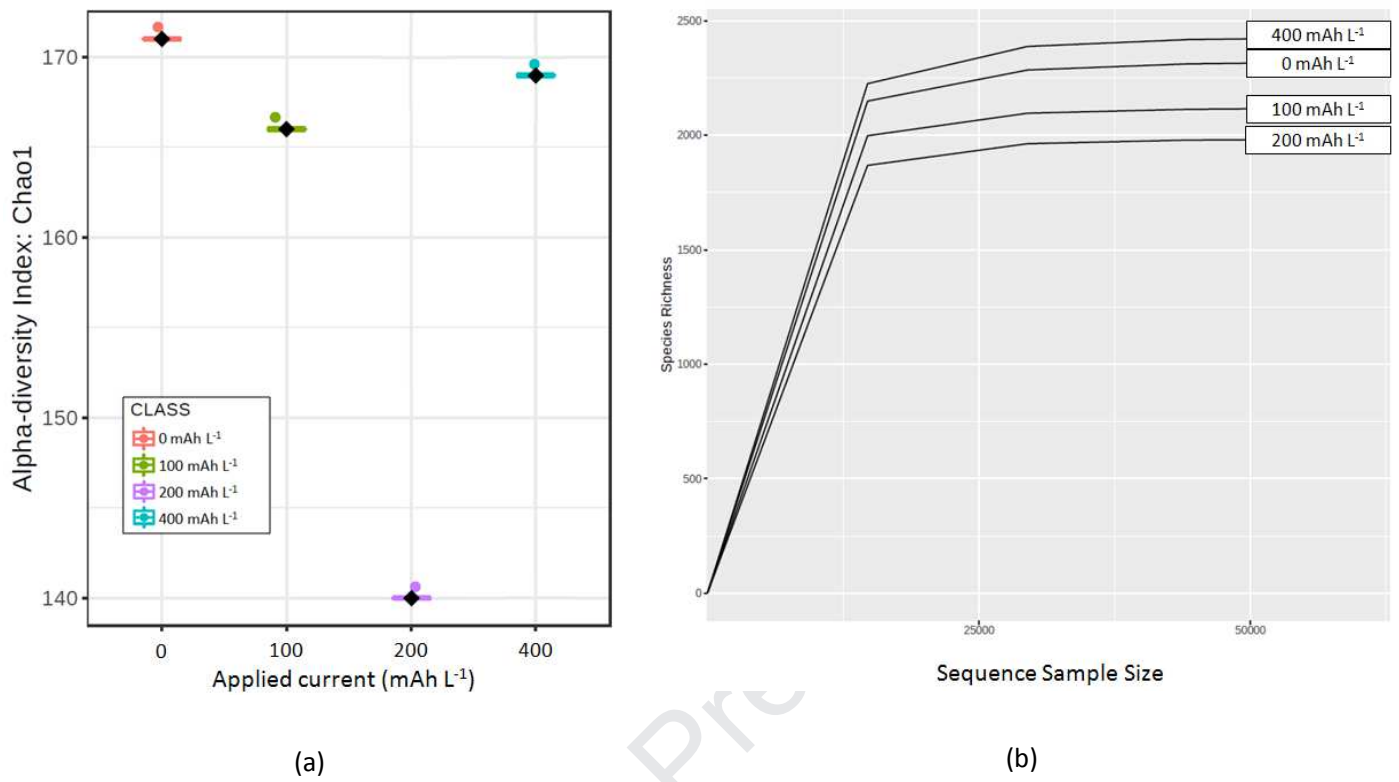


Figure 7 (a) Alpha-diversity (Chao1) and (b) rarefaction curves of mixed liquor samples collected from the different Electro-MBR's operating conditions

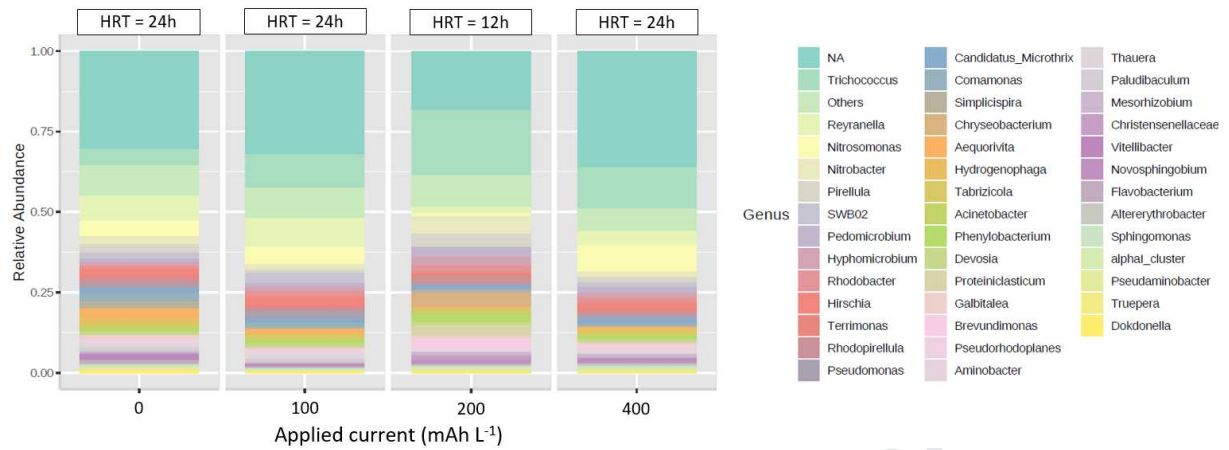


Figure 8 MBR's and Electro-MBR's mixed liquor microbial population structure at the genus level

**Highlights:**

- Nitrate cathodic reduction rate depends on the cathode material's hydrogen overpotential
- Ferric ion dosage of 82 to 325 mg Fe L<sup>-1</sup> has shown no nitrification inhibition phenomena
- Nitrification inhibition is avoided by the use of a platinized titanium cathode
- Nitrosomonas relative abundance is positively correlated to the charge loading
- A Ti/Pt-Fe Electro-MBR can simultaneously remove >99% of NH<sub>4</sub> and P<sub>tot</sub> at 400 mAh L<sup>-1</sup>

**Declaration of interests**

The authors declare that they have no known competing financial interests or personal relationships that could have appeared to influence the work reported in this paper.

The authors declare the following financial interests/personal relationships which may be considered as potential competing interests: